Wireless channel characterization and modeling in oil and gas refinery plants

Stefano Savazzi[1], Sergio Guardiano[3], Umberto Spagnolini[2]
[1]National Research Council (CNR), IEIIT institute, Milano, [2]DEI, Politecnico di Milano, [3]Saipem S.p.A. - A subsidiary of Eni S.p.A., San Donato, Italy.
E-mail: stefano.savazzi@cnr.it, spagnoli@elet.polimi.it, Sergio.Guardiano@saipem.com

***Abstract*— Wireless network technology is becoming a remarkable research topic in the field of industrial monitoring and process control. The widespread adoption of the wireless systems is mandatorily paired with the development of tools for prediction of the wireless link quality to mimic network planning procedures similar to conventional wired systems. In industrial sites the radio signals are prone to blockage due to highly dense metallic structures. The layout of scattering objects from the infrastructure influences the link quality, and thus the strength of the signal power. In this paper it is developed a novel channel model specifically tailored to predict the quality of the radio signal in environments affected by highly dense metallic building blockage. The propagation model is based on the diffraction theory and it makes use of the 3D model of the plant to classify the links based on the number and the density of the obstructions surrounding each link. The proposed channel modeling approach is validated by experimental measurements in two oil refinery sites using industry standard ISA SP100.11a compliant commercial devices operating at 2.4GHz.**

I. Introduction

The adoption of wireless sensor networks in an industrial context has lately become a strategic issue for most manufacturing companies. The status of current technology allows the deployment of low power, cost effective network nodes in a battery powered configuration which substitute the traditional wired devices in a very cost effective way [1]. The installation of wireless sensors may give significant cost savings for a variety of typical plants [2]. Current wireless networks for industrial control and monitoring are based on the IEEE 802.15.4 standard [3] and are typically considered for monitoring tasks and supervised/regulatory control. Typical locations of wireless devices used for remote control and monitoring of industrial oil and gas refinery sites are characterized by harsh environments where radio signals are prone to blockage and multipath fading due to metallic structures (structural pipe racks, metallic towers and buildings, etc...) that obstruct the direct path [4].

With the widespread use of the wireless technology in industrial environments, the development of virtual (computer aided) network planning software tools is now becoming crucial for accurate system deployment. Inaccuracies during the radio planning design phase will turn into issues during the commissioning phase. As an example, deploying new wireless devices to improve the coverage as well as moving around some wired nodes such as gateways and/or access points might require to re-open excavations along the cable route

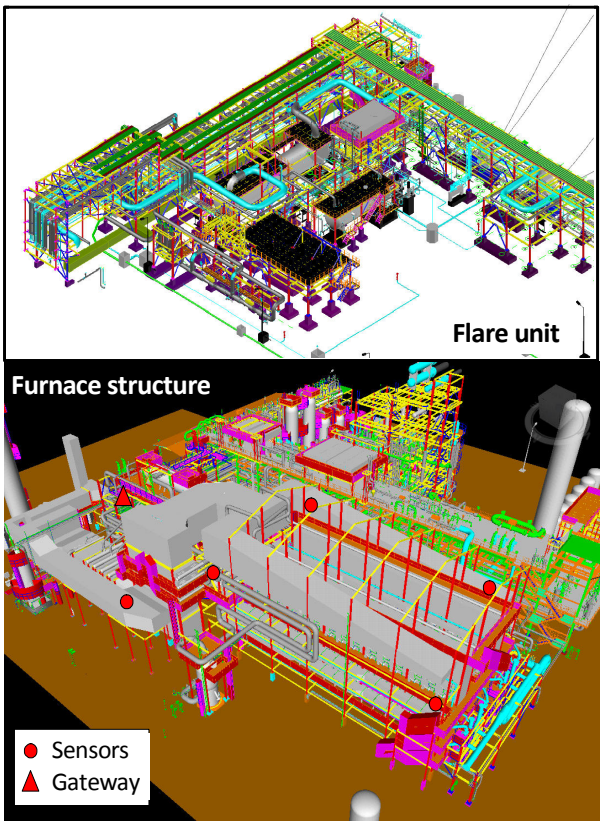

Fig. 1. 3D-CAD model of the industrial sites for testing: Flare unit (on top) and Furnace structure (at bottom).

which is totally unacceptable during the commissioning (or even pre-commissioning) phase of the plant. Accurate network planning limits the need to oversize the design of the overall system (which is obviously an extra cost for the contractor). Therefore, it is crucial to develop consistent design guidelines and tools that can allow to achieve a reasonable accuracy in the prediction of the wireless coverage. Making use of the 3D model (if available) during the design phase is also of utmost importance to achieve this result. An example of a 3D view of two oil refinery sites is illustrated in Fig. 1: the wireless devices (herein referred to as sensors) can be connected by star or mesh mode towards a gateway device collecting data and re-routing to a wired network. Network planning is based on the prediction of the pairwise wireless link qualities

among all the devices in the distributed network: the link quality is expressed in terms of the strength of the received signal. The prediction can be supported by independent radio measurement campaigns over typical refinery environments and/or by models based on propagation theory and statistical or ray-tracing tools.

Conventional empirical channel models [5] cannot fully capture the unique propagation characteristics of the industrial environments, in addition the ray-tracing based models [6] turn out to be not practicable to process the large amount of structures over large industrial sites. This motivates the development of accurate site-specific channel models based on a small fraction of measurements taken in the refinery area [7].

Contribution of the paper. In this paper a novel empirical channel model based on the theory of diffraction is proposed to assess the link quality in radio environments affected by highly dense metallic building blockage. The wireless links are partitioned into mutually exclusive classes: for each class a separate channel model is proposed to predict the quality of the radio link. The link classification is based on the analysis of the characteristics of the obstructions that impair the wireless propagation. The 3D-CAD model of the refinery site (see Fig,. 1) is used to identify the structure of the building blockage. Although the channel modeling and the classification methodology proposed in this paper are fairly general and applicable in different scenarios, in order to exhibit practical and highly focused results, the model is validated by experimental measurements using industry standard ISA SP100.11a compliant [8] devices operating at 2.4GHz based on the IEEE 802.15.4-2006 physical layer. Measurement campaigns are carried out in two sites located in a large-size oil refinery plant.

II. Channel modeling

A typical industrial environment shows relevant similarities with a dense urban microcellular site characterized by an harsh environment for short-range (10-150m) propagation with metallic structures [4], changing environmental conditions, non-line of sight (NLOS) and possible co-located wireless applications running over the same unlicensed spectrum. The wireless links without a clear line-of-sight (LOS) path undergo more severe received signal power attenuations than those where the LOS path is unobstructed. This additional attenuation is almost uncorrelated with the distance between the transmitter and the receiver [9]. The main scatterers/objects that are responsible for the received signal power attenuation are mostly confined within the first and second Fresnel zones as these can be considered to contribute to the main propagating energy in the wavefield. For a wireless link where the direct path between transmitter and received has length d, the n-th Fresnel zone is the region inside an ellipsoid with circular cross-section. The radius of the n-th Fresnel zone at distance $q \leq d$ is $r_n(q) = \sqrt{n\lambda q(d-q)d^{-1}}$ with $\lambda = 0.125m$ the signal wavelength.

We assume that any two wireless devices (a, b) are deployed at fixed locations and are equipped with radio devices characterized by single omnidirectional antenna transceivers. As for typical scenarios, the gateway antenna is mounted on an elevated point while flat terrain is assumed. The propagation model describes the correlation between the size of the (mostly metallic) obstructions located within the Fresnel volumes and the total received signal strength (RSS) experienced along the propagation path. The RSS is thus the metric used to assess the quality of the radio link: it combines a LOS component and an excess attenuation that accounts for building blockage. The general model for the RSS experienced by a wireless link $\gamma_{a,b} = s \times g_{a,b}$ consists of: *i)* a random term s with $\mathrm{E}[s] = 1$ accounting for the fluctuations of the received power[1]; *ii)* a deterministic and distance-dependent component $g_{a,b} = g_{a,b}(d)$ (in dB scale)

$$g_{a,b}|_{db} = g_0 - 20\log_{10}(1 + d/d_0) - \\ - 10(\alpha - 2)\log_{10}(1 + d/d_F) - \sigma \quad (1)$$

where $g_0 = g_0(P_T, d_0)$ is the channel gain function of the transmit power P_T, and measured at a reference distance d_0 ($d_0 = 2$m typical); α is the path-loss exponent while

$$d_F = 2h_a h_b/\lambda \quad (2)$$

is the Fresnel distance being a function of the antenna heights from the ground h_a and h_b of devices a and b, respectively. The term σ denotes the additional signal attenuation that depends on size and density of the metallic objects located within the Fresnel volume, i.e., blocking the line-of-sight path. A model to characterize this additional attenuation component is derived in Sect. 2.B. Path loss exponent is typically set to $\alpha = 2$ in short range environments [9] where ground reflections can be neglected, for $d < d_F$. Larger path loss exponents $\alpha > 2$ are caused by reflections from the ground and can be experimented in long-range cases for $d > d_F$. The reflection of the radio signals from the flat terrain does not influence the attenuation parameter σ but only the path-loss exponent α. A similar model has been also proposed in [9] and it is validated here by measurements over the refinery sites (see Sect. 4).

The probability P_E of successful communication depends on the random fluctuations of the RSS. Successful communication is modeled by outage probability such that $P_E = \Pr[\gamma_{a,b} \geq \beta]$. The threshold β is typically set to $\beta = -85dBm$ such that $P_E \leq 10^{-6}$ [3]. Any link experiencing $\gamma_{a,b} < \beta$ is assumed as unreliable and thus it should not be considered during network planning.

A. Diffraction model for prediction of building blockage

In the proposed model, it is assumed that the additional attenuation σ in (1) is due to the diffraction from the building blockage consisting of metallic obstacles with different dimensions and acting as absorbing interfaces.

The diffraction model for the building blockage term σ is based on the Fresnel-Kirchhoff method and it is valid for perfectly absorbing obstacles [10]. The attenuation σ in (1) is obtained as a function of the received field E

$$\sigma = -20\log_{10}|E/E_{free}|. \quad (3)$$

[1] with typical standard deviation below $5dB$ in static environments.

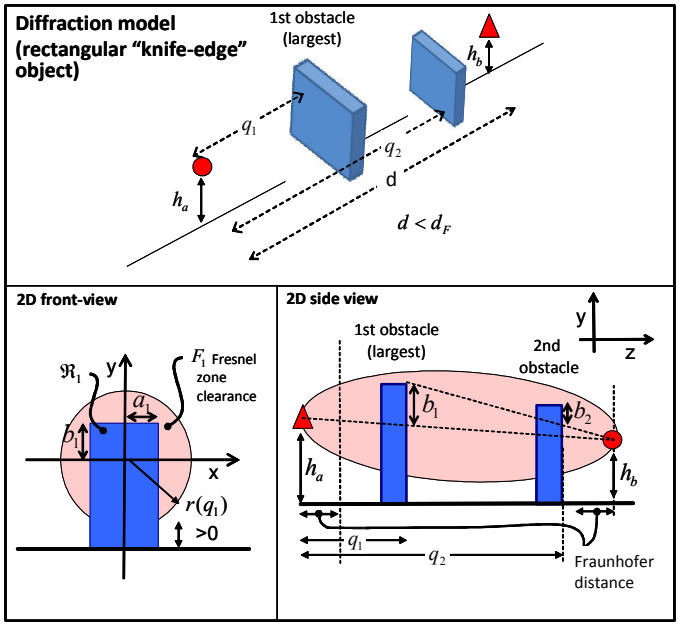

Fig. 2. Fresnel-Kirchhoff method for modeling the attenuation caused by 2D rectangular "knife-edge" absorbing objects.

The ratio E/E_{free} describes the obstruction loss in excess of the free space field loss E_{free}. Large-size metallic objects obstructing the wireless link absorb a large amount of signal power and limit the received field to a small fraction $E/E_{free} \ll 1$ of the one that would be observed under free-space propagation. A simplified description of the propagation environment (with 2 obstacles) is considered in Fig. 2. To simplify the reasoning, we assume that the obstacles surrounding the transmitter and the receiver antennas lie in the far-field region, in addition the shape of the obstacles obstructing the Fresnel zones is square or rectangular. Shapes that are more typical in refinery sites (tubes, structural pipe-racks etc...) have been approximated as discussed in [11] (extension not covered here due to space limits). For the i-th object, the zone clearance $\mathcal{F}_i$ in the (x,y) plane denotes the region of the Fresnel volume circular section that is free from obstacles. The shaded region $\mathcal{R}_i$ in the same plane indicates instead the complementary portion of the surface occupied by the obstacle.

The Fresnel-Kirchhoff approach to model the obstruction loss $E(q_i)/E_{free}$ caused by a single i-th obstacle located at distance $q_i \leq d$ is based on the Huygen's principle and can be applied in a mathematical form to predict the actual field strength diffracted by one obstacle modeled as a knife-edge. The model can be extended to 2D to take into account both the lateral and the vertical profiles of the obstruction by integrating the exponential phase term of the wavefield over the two dimensions [10]. From Fig. 2, the loss $E(q_i)/E_{free}$ can be approximated for $(x,y) \ll q_i, d-q_i$ as

$$\left|\frac{E(q_i)}{E_{free}}\right| = \left|1 - j\int_{(x,y)\in\mathcal{R}_i} \frac{1}{r_1^2(q_i)} \exp\left[\frac{-j\pi\left(x^2+y^2\right)}{r_1^2(q_i)}\right] dxdy\right|, \quad (4)$$

where $r_1(q_i)$ approximates the radius of the 1st Fresnel volume circular section[2] corresponding to the location of the obstruction. Closed form and exact solutions for the integral (4) can be found in [12].

The model (4) is extended to multiple obstacles by following the Deygout method [12]. The overall loss E/E_{free} in (3) for $B > 1$ obstacles is obtained by multiplying each contribution along the LOS path so that $E/E_{free} = \prod_{i=1}^{B} E(q_i)/E_{free}$. For multiple obstacles the lateral a_i and vertical b_i dimensions of the region $\mathcal{R}_i$ for the i-th obstacle (see Fig. 2) are calculated with respect to the size of the largest obstacle (e.g., obstacle $i = 1$ in Fig.2).

III. Wireless Link Classification

The proposed approach to the evaluation of the pairwise link channel qualities makes use of a database of radio measurements taken in different refinery sites. The measurements are used to define 5 mutually exclusive link categories that take into account the different sizes and the positions of the most relevant obstructions inside the (1st and 2nd) Fresnel volumes surrounding the considered links. Each link type is thus characterized by a specific configuration of the Fresnel zone clearance that corresponds to a reference value for the obstruction loss E/E_{free} according to the model outlined in Sect. 2.B. The analysis of the building blockage property is based on the inspection of the full 2D/3D model of the plant. For each link type ℓ, the reference attenuation $\sigma(\ell)$ used to predict the link quality in (1) is computed as in (3).

Based on the experimental activity, five different link types are considered (see Fig. 3).

Type I: LOS ($\ell = 1$) link type is characterized by the absence of obstacles (with dimensions larger than the signal wavelength λ) within the 1st Fresnel volume, while obstacles might instead occupy the remaining Fresnel volumes. The nominal[3] range to guarantee a reliable connection is found as $R \simeq 150m$ (for RSS above $\beta = -85$dBm). From equation (4), in the worst-case scenario where obstacles completely obstruct the n-th Fresnel volumes with $n \geq 3$, the observed received electric field is the $E/E_{free} = 90\%$ of the one that would be measured in the free-space case (thus corresponding to an attenuation of $\sigma(\ell) \simeq 1dB$ [13]).

Type II: near-LOS ($\ell = 2$) link type is observed in environments where the obstacles are located in the first Fresnel outer region at distance $0.6 \times r_1(q)$ from the direct path. The shaded sub-region in Figure 3 can be considered as a 'forbidden' region: if this region is kept clear then the total path attenuation will be practically the same as in the unobstructed case. This clearance zone is thus used here as a criterion to decide whether an object is to be treated as a relevant obstruction. The radio propagation for this link category is characterized by an additional signal energy loss compared to Type I. Based on the radio measurement campaigns and the diffraction model in (4), the Type II links typically retain the $E/E_{free} = 70\%$ of the received field observed in the free space case. The theoretical maximum range reduces to $R \simeq 108m$.

[2]The approximation uses the distances measured along the ground rather than along the direct wave.

[3]such that $\mathrm{E}[\gamma_{a,b}] \geq \beta$

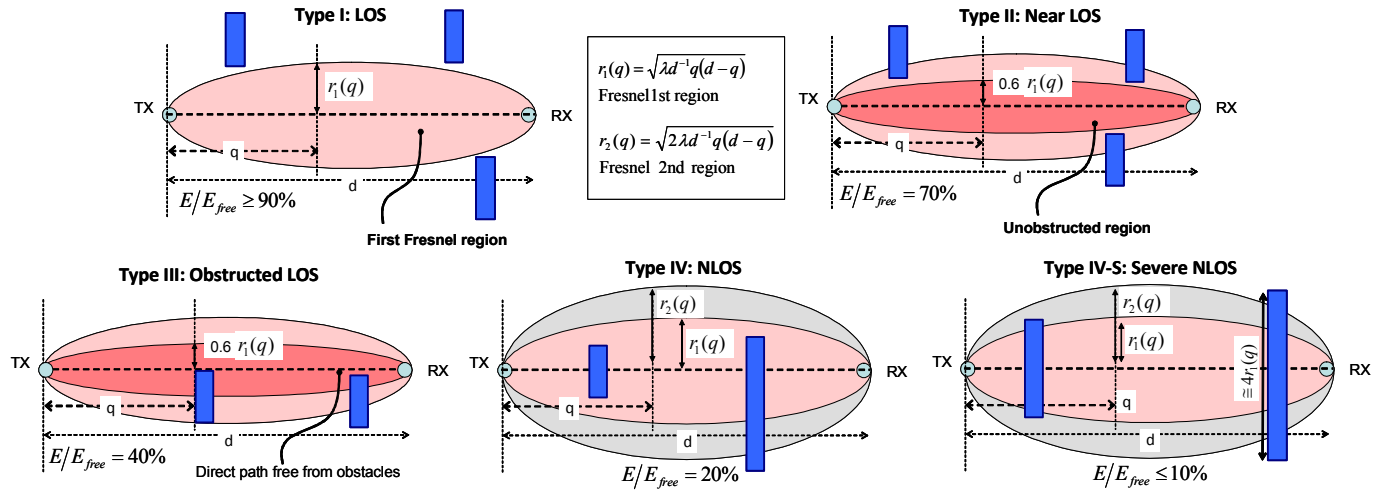

Fig. 3. Proposed link classification and Fresnel clearance zones

Type III obstructed-LOS ($\ell = 3$) link type is observed in environments where obstacles are located inside the forbidden region, although the direct path connecting the transmitter and the receiver is still completely unobstructed. The links belonging to this category hold approximately the $E/E_{free} = 40\%$ of the received field experienced in the free space case. The theoretical maximum range is $R \simeq 60m$.

Type IV NLOS ($\ell = 4$) link type is characterized by objects obstructing the direct path between transmitter and receiver: the size of those objects is such that a clearance zone is still visible, $\bigcap_i \mathcal{F}_i \neq \varnothing$, suggesting that there might be the possibility of reliable communication. Being the forbidden region and the LOS path both obstructed, a reasonable value for the loss is found as $E/E_{free} = 20\%$. The theoretical maximum range further reduces to $R \simeq 32m$.

Type IV-S severe-NLOS ($\ell = 5$) link type refers to a severe NLOS environment where the first Fresnel region is *completely* obstructed by one or more obstacles with significant size (scaling as $\sim 4 \div 5 r_1(q)$) so that the observed received field falls below the $E/E_{free} = 10\%$ of the one that would be measured in the free-space case. The theoretical maximum range is $R \simeq 15m$. This model type resembles a propagation environment where the LOS path is blocked by large-size concrete buildings [9].

IV. Experimental activity

In the proposed experimental set-up, we deployed 3 absolute and gauge pressure transceivers communicating periodically (with refresh rate of 1min.) with a Gateway node by star topology. Compared to mesh topology, a star topology network provides better performance in terms of real-time responsiveness which are required in the plant. Radio transmitters conform with the ISA SP100.11a protocol [8] with radio transmit power set to $P_T = 11.6dBm$. The antennas are vertically polarized and omnidirectional with gain 2dBi: antennas with such gain can be commonly found on the market and do not require special alignments. The experiments have been carried out in two sites within an oil refinery: the first site is a 100mx200m area around a flare unit, the second one is a 60mx30m area surrounding a furnace structure. All the environments under consideration are characterized by metallic objects and concrete buildings with high reflectivity surfaces. Before the test we used a signal analyzer to characterize the interferers in the area. Since no interference was detected, the IEEE 802.15.4 channels selected for the experiments have center frequencies 2.405 GHz and 2.480 GHz, corresponding to the ISA SP100 channel numbers 1 and 15, respectively. The value of the channel gain g_0 under free-space propagation at reference distance $d_0 = 2m$ is found during the calibration stage as $g_0 = -47dBm$ for all the devices.

In all of the considered short range cases for $d < d_F$, the measured path loss exponent is found as $\alpha = 2$ while the additional attenuation σ depends on the density of the obstacles according to the link classification described in Sect. 3. Propagation over long ranges such that $d > d_F$ suffers from a larger path-loss due to ground reflections. The signal attenuation σ characterizing each link is calculated by first identifying the number and size of objects that block the direct path between the transmitter and receiver pair compared to the Fresnel zones. The link classification stage is then performed by inspection of the 2D/3D maps of the sites. The radio propagation for the chosen link category is modeled as outlined in Sect. 2. The measurements analyzed in the following sections highlight the accuracy of the proposed channel characterization and modeling approach.

A. Site test #1: Flare unit

In this test the gateway is mounted in 4 different locations corresponding to different deployment cases as illustrated in the floor plan maps of Fig. 4. For deployment case #1 the height from the ground of the gateway is $1.5m$ ($d_F \simeq 25m$), for the remaining cases the height is above $6m$ ($d_F \simeq 50m$). For all cases the 3 sensors labelled as B, C and D are moved in different positions labeled by lower-case letters (a, b, c). The corresponding average RSS measurements are reported by circle markers for all the deployment cases and

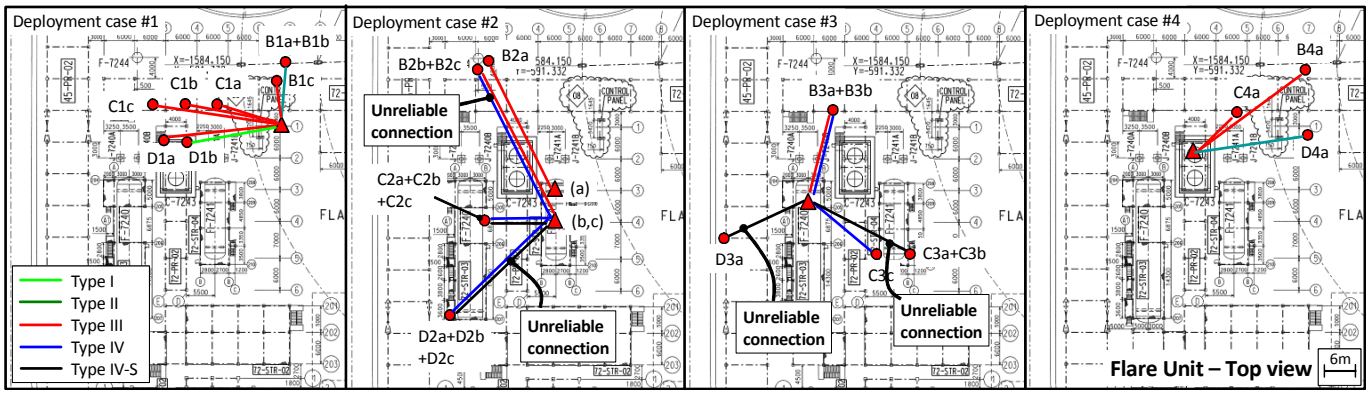

Fig. 4. Flare unit test sites and link classification according to the cathegories defined in Sect. 3. Links are colored based on the selected link type, unreliable links are also highlighted

analyzed in Fig. 5. Markers have different colors to identify the link category while link classification is based on the inspection of 2D and 3D-CAD maps (see Fig. 1 on top). The double sided arrow symbols identify the test locations where device height was increased/decreased of approx. $1m$. The predicted propagation model for each link category (Sect. 3) is superimposed to the measurements by solid lines, using the same color code to highlight the prediction accuracy.

The effectiveness of the proposed channel characterization and modeling approach can be appreciated in several settings. To highlight a relevant example, in the deployment case 3 the transmitters located at positions C3a (ground level) and C3b (1m height from ground) are hidden behind a big cylindrical vessel (see Fig. 4) that completely obstruct the 1st Fresnel region. The wireless links connecting to the Gateway retain the $E/E_{free} = 13\%$ and the $E/E_{free} = 9\%$, of the field that would be measured in free space, respectively. Therefore, they can be reasonably classified as Type IV-S. As confirmed by measurements, the predicted RSS is below the critical $\beta = -85$dBm reliability threshold (distance $d = 26m$) suggesting the need for a repeater acting as relay. The same transmitter is now moved at position C3c to circumvent the large obstruction and create more favorable propagation conditions. In this case, by inspection of the 3D map the 1st Fresnel region is slightly unobstructed: the link retains a larger fraction ($E/E_{free} = 17\%$) of field and thus can be reasonably classified as Type IV. As confirmed by the chosen model, the connection with the Gateway is now reliable as RSS -82dBm.

A long-range test have been also carried out with the Gateway located in the same position of case 4 while the device C on ground was moved in two sites. The first one was an open area classified as near LOS environment (Type II) on the right side of the Flare unit at distance 109m from the Gateway, the second site was located at distance 132m from the Gateway in the southern part of the Flare unit where the LOS path is obstructed by a building. Path loss caused by the ground reflections (flat terrain) can be reasonably modeled as in (1) with exponent $\alpha = 2.5$. For the first test, the wireless link is characterized by $E/E_{free} = 83\%$. The measured RSS of $-85dBm$ confirms the predicted range for the corresponding Type II link category (see Section 3). In

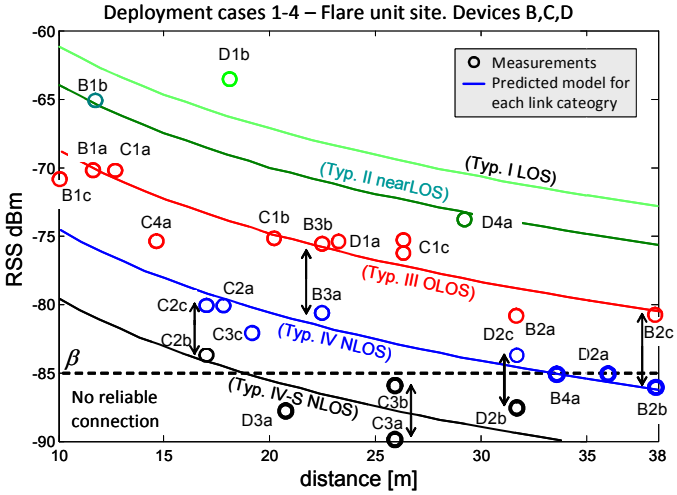

Fig. 5. RSS measurements (circle markers) for devices B, C and D over the Flare unit sites (1-4). Positions of devices are indicated by lower-case letters and corresponds to the maps in Fig. 4. Colors identify the chosen link cathegory. Predicted model for each link category is superimposed by solid lines, using the same color code. The double sided arrow symbols identify the test locations where device height was modified (approx +1m).

the second test the link only retains the $E/E_{free} = 44\%$ of the free space field (the attenuation caused by the building is $7dB$) and is classified as unreliable as the RSS is $-91dBm$.

B. Site test #2: Furnace structure

In this test the gateway is mounted on the stairway in the south-east of the furnace around $10m$ above the ground level. In this scenario devices C and D are moved over four different floors of the furnace structure according to Fig. 6. Device B instead is located on ground, at 5 positions in front of the furnace structure. The distance between each device and the gateway ranges between 14m and 57m and is lower than the Fresnel distance $d_F \simeq 80m$ in all cases. Measurements and predicted model for each link category are reported in Fig. 7 using the same color code adopted for the Flare unit scenario. By inspection of the 2D and 3D maps of the site, the links corresponding to positions B5(d and e), D5e and C5a can

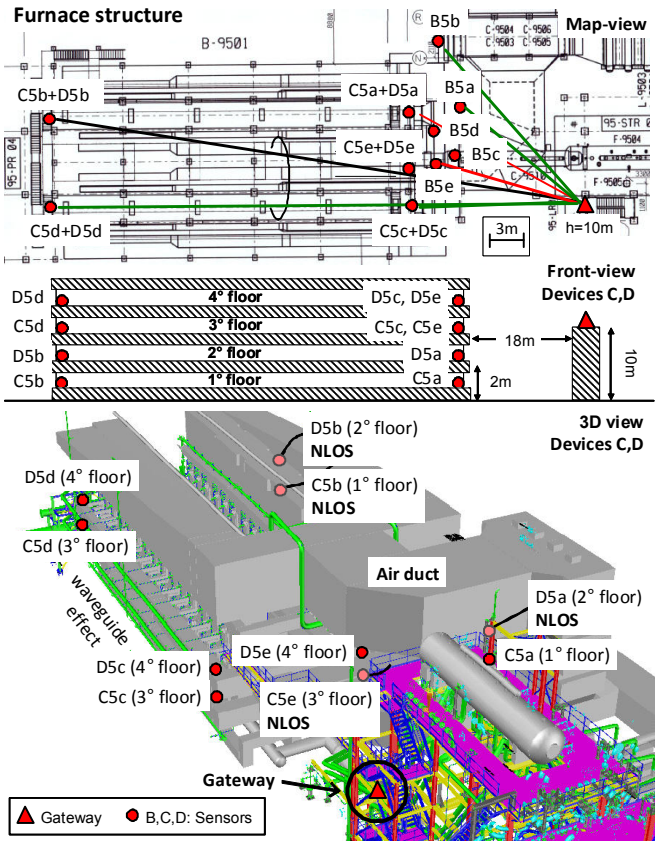

Fig. 6. Furnace structure test site: top and front-view (top) and 3D view (bottom) of the environment.

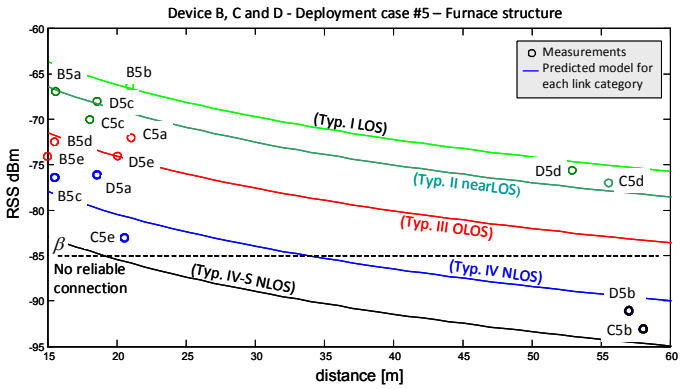

Fig. 7. RSS measurements (circle markers) and predicted model (solid lines) for the furnace site. Same color code as for Fig. 5.

be reasonably classified as Type III ($E/E_{free} = 40\%$, or $\sigma(\ell = 3) \simeq 8dB$), being the forbidden region defined in Fig. 2 partially obstructed. Measured attenuations are ranging from $\sigma = 5 \div 10dB$ and confirm this choice. The NLOS links (Type IV) corresponds to positions B5c, D5a and C5e with observed attenuation ranging from $\sigma = 11 \div 17dB$. For positions D5d (4rd floor) and C5d (3rd floor), the metallic structure produces a waveguide effect on propagation such that reliable communication occurs even across the whole furnace structure: the wireless signals propagate all around the furnace environment without obstacles and take advantage of the constructive interference. The positions D5b (2rd floor) and C5b (1rd floor) are instead surrounded by the furnace building that fully obstructs the 1st Fresnel volume and absorbs approximately the 84% and the 88% of the free space field, with $E/E_{free} = 16\%$ and $E/E_{free} = 12\%$, respectively (Type IV-S). As confirmed by measurements, the predicted RSS for Type IV-S link (with distance $d = 57m$) is below the critical $-85dBm$ reliability threshold: a repeater is therefore required to relay the signal transmitted from positions D5b and C5b towards the Gateway node.

V. Concluding Remarks

In this paper a novel empirical channel model based on the theory of diffraction is proposed to characterize the wireless propagation in industrial environments. The wireless links are partitioned into mutually exclusive classes based on the 3D structure of the building blockage that characterizes the amount of obstruction loss. For each class a separate channel model is proposed to predict the quality of the radio link. The proposed classification approach is validated by experimental measurements in critical areas within an oil refinery plant characterized by highly dense metallic structure. Industry ISA SP100.11a standard devices operating at 2.4GHz are adopted. Preliminary results from the surveys confirm the effectiveness of the proposed method as it provides a practical tool for virtual network planning with reasonable accuracy.

References

[1] A. Willig, "Recent and emerging topics in wireless industrial communications: a selection," IEEE Trans. on Ind. Inform., vol. 4, no. 2, May 2008.

[2] S. Savazzi, S. Guardiano, U. Spagnolini, "Wireless Critical Process Control in oil and gas refinery plants," Proc. of IEEE International Conference on Industrial Technology, Greece, March 2012.

[3] Standard IEEE 802.15.4-2006, "Part 15.4: Wireless MAC and PHY specifications for low-rate Wireless Personal Area Networks, " 2006.

[4] L. Tang, et al., "Channel Characterization and Link Quality Assessment of IEEE 802.15.4-Compliant Radio for Factory Environments," IEEE Trans. on Ind. Inform., vol. 3, no. 2, May 2007.

[5] V. Erceg, et al. "An empirically based path loss model for wireless channels in suburban environment," IEEE Trans. on Automat. Contr., vol. 17, pp. 1205-1211, Jul. 1999.

[6] S. J. Fortune et al. "Wise design of indoor wireless system: practical computation and organization," IEEE Computational Science and Engineering, vol. 2, pp. 58-68, Mar. 1995.

[7] J. Lei, L. Greenstein, R. Yates, "Link gain matrix estimation in distributed wireless networks," Proc. of IEEE GLOBECOM New Orleans, USA, Dec. 2008.

[8] Standard ISA100.11a-2009 "Wireless systems for industrial automation: process control and related applications," ISA, July 2009.

[9] D. J. Y. Lee and W. C. Y. Lee, "Propagation prediction in and through buildings," IEEE Trans. on Vehicular Technology, vol. 49, no. 5, Sept. 2000.

[10] H. Mokhtaru, P. Lazaridis, "Comparative study of lateral profile knife-edge diffraction and ray tracing technique using GTD in urban environment," IEEE Trans. on Vehicular Tech., vol. 48, no. 1, Jan. 1999.

[11] A. Nyuli, B. Szekeres, "An improved method for calculating the diffraction loss of natural and man-made obstacles," Proc. of PIMRC, pp.426-430, Oct 1992.

[12] C. L. Giovanelli, "An analysis of simplified solutions for multiple knife-edge diffraction," IEEE Transactions on Antennas and Propagation, vol. 32 no. 3, pp.297–301, 1984.

[13] G. E. Athanasiadou, "Incorporating the Fresnel zone theory in ray tracing for propagation modelling of fixed wireless access channels," Proc. of PIMRC, pp. 3-7 Sept. 2007.